

# Decay Properties of $D$ and $D_s$ mesons

<sup>1</sup>Bhavin Patel and \*P C Vinodkumar

LDRP- Institute of Technology and Research, Gandhinagar- 382 015, Gujarat, INDIA.

\*Department of Physics, Sardar Patel University, Vallabh Vidyanagar- 388 120, Gujarat, INDIA

## Abstract

The decay rates and spectroscopy of the  $D$  and  $D_s$  mesons are computed in a nonrelativistic phenomenological quark-antiquark potential of the type  $V(r) = -\frac{4}{3}\frac{\alpha_s}{r} + Ar^\nu$  with different choices of  $\nu$ . Numerical method to solve the Schrödinger equation has been used to obtain the spectroscopy of  $q\bar{Q}$  mesons. The spin hyperfine, spin-orbit and tensor components of the one gluon exchange interactions are employed to compute the spectroscopy of the excited  $S$  states, low lying  $P$ -waves and  $D$ -waves. The numerically obtained radial solutions are employed to obtain the decay constant and leptonic decay widths. It has been observed that predictions of the spectroscopy and the decay widths are consistent with other model predictions as well as with the known experimental values.

## 1 Introduction

Spectroscopy of hadrons containing heavy flavours has attracted considerable interest in recent years due to many experimental facilities such as the BES at the Beijing Electron Positron Collider (BEPC), E835 at Fermilab, and CLEO at the Cornell Electron Storage Ring (CESR) *etc.*, worldover. They have been able to collect huge data samples in the heavy flavour sector. Where as B-meson factories, BaBar at PEP-II and Belle at KEKB are working on the observation of new and possibly exotic hadronic states. All these experiments are capable of discovering new hadrons, new production mechanisms, new decays and transitions and in general will be providing high precision data sample with better statistics and higher confidence level. After having played a major role in the foundation of QCD, heavy hadron spectroscopy has witnessed in the last few years a renewal of interest led by the many new data coming from the B factories, CLEO and the Tevatron and by the progress made in the theoretical methods. The remarkable progress at the experimental side, with various high energy machines such as BaBar, BELLE, B-factories, Tevatron, ARGUS collaborations, CLEO, CDF,  $D\bar{D}$  *etc.*, for the study of hadrons has opened up new challenges in the theoretical understanding of light-heavy flavour hadrons. The existing

---

<sup>1</sup>Email: azadpatel2003@gmail.com

results on excited heavy-light mesons are therefore partially inconclusive, and even contradictory in several cases. The predictions of masses of heavy-light system for ground state as well as excited state are few from the theory [1, 2, 3, 4, 5, 6, 7]. In the open charm sector, the observation of a charm-strange state, the  $D_{sJ}^*(2317)$  state [8] by BaBar Collaboration. It was confirmed by CLEO Collaboration at the Cornell Electron Storage Ring [9] and also by Belle Collaboration at KEK [10]. Besides, BaBar had also pointed out to the existence of another charm-strange meson, the  $D_{sJ}(2460)$  [8]. This resonance was measured by CLEO [9] and confirmed by Belle [10]. Belle results [10] are consistent with the spin-parity assignments of  $J^P = 0^+$  for the  $D_{sJ}^*(2317)$  and  $J^P = 1^+$  for the  $D_{sJ}(2460)$ . Thus, these states are well established and confirmed independently by different experiments. They present unexpected properties, quite different from those predicted by quark potential models. If they would correspond to standard  $P$ -wave mesons made of a charm quark and a strange antiquark their masses would be larger [11], around 2.48 GeV for the  $D_{sJ}^*(2317)$  and 2.55 GeV for the  $D_{sJ}(2460)$ . They would be therefore above the  $DK$  and  $D^*K$  thresholds, respectively with being broad resonances. However the states observed by BaBar and CLEO are very narrow,  $\Gamma < 4.6$  MeV for the  $D_{sJ}^*(2317)$  and  $\Gamma < 5.5$  MeV for the  $D_{sJ}(2460)$ .

In near future, even larger data samples are expected from the BES-III upgraded experiments, while the B factories and the Fermilab Tevatron will continue to supply valuable data for few more years. Later on, the LHC experiments at CERN, Panda at GSI *etc.*, will be accumulating large data sets which will offer greater opportunities and challenges particularly in the field of heavy flavour physics [12].

At the hadronic scale the nonperturbative effects connected with complicated structure of QCD vacuum necessarily play an important role. But our limited knowledge about the nonperturbative QCD leads to a theoretical uncertainty in the quark- antiquark potential at large and intermediate distances [13]. So a successful theoretical model can provide important information about the quark-antiquark interactions and the behavior of QCD at the hadronic scale. Though there exist many potential models with relativistic and nonrelativistic considerations employed to study the hadron properties based on its quark structure [14, 15, 16, 17, 18, 19, 20, 21, 22, 23, 24, 25, 26, 27, 28], the most commonly used potential is the coulomb plus linear power potential,  $V(r) = -\frac{4}{3}\frac{\alpha_s}{r} + \sigma r$ , with the string tension  $\sigma$  [29, 30]. However, for the higher excited mesonic states it is argued that the string tension  $\sigma$  must depend on the  $Q\bar{Q}$  separation [31, 32]. This corresponds to flattening of the confinement potential at larger  $r$  ( $r \geq 1fm$ ). More over the analysis based on Regge trajectories for meson states suggests the confinement part of the potential to have the power  $\frac{2}{3}$  instead of 1 [33, 34]. This has prompted us to choose a power form for the confining part of the interquark potential and study the properties of heavy flavour systems by varying the power of the confinement part of the interquark potential different from 1.0.

Apart from the spectroscopic predictions of higher orbital states, other problems associated with the phenomenological models employed for the properties of mesons are the right predictions of their decay properties. For better predictions of the decay widths, many models need to incorporate additional terms such as the radiative contributions, higher order QCD corrections *etc.*, to the conventional decay formula [14, 15, 35, 36, 37].

The decay widths can provide an account of the compactness of the meson system in terms of the radial wave function which is an useful information complementary to spectroscopy [38]. Other unresolved issues are related to the hyperfine and fine structure splitting of the mesonic states and their intricate dependence with the constituent quark masses and the running strong coupling constant. Thus, in this paper we make an attempt to study properties like mass spectrum, decay constants and other decay properties of the open charm mesons ( $D, D_s$ ). We investigate the heavy-light mass spectra of  $D(c\bar{q})$  and  $D_s(c\bar{s})$  mesons in the frame work of the nonrelativistic  $CPP_\nu$  potential model. In the present study, we consider different choices of the potential power index  $\nu$  in the range  $0.1 < \nu < 2.0$ .

## 2 Nonrelativistic Treatment for Heavy Flavour Mesons using $CPP_\nu$

In general, properties of heavy flavour mesons have been studied based on potential models in the frame work of relativistic as well as nonrelativistic quantum mechanics. In the limit of heavy quark mass  $m_Q \rightarrow \infty$ , heavy meson properties are governed by the dynamics of the light quark. As such, these states become hydrogen like atoms of hadron physics. Moreover, both the non-relativistic predictions are in fair agreements with each other as well as with the available experimental and lattice results. Hence, for the present study of charm meson bound states, we consider a nonrelativistic Hamiltonian given by [14, 15, 39, 40, 41, 42]

$$H = M + \frac{p^2}{2M_1} + V(r), \quad (1)$$

here,

$$M = m_1 + m_2, \quad \text{and} \quad M_1 = \frac{m_1 m_2}{m_1 + m_2}, \quad (2)$$

The relative momentum of each quark is represented by  $p$  and  $V(r)$  is the quark-antiquark potential. Nonrelativistically, this interaction potential consists of a central term  $V_c(r)$  and a spin dependent part  $V_{SD}(r)$ . The central part  $V_c(r)$  is expressed in terms of a vector (Coulomb) plus a scalar (confining) part given by

$$V_c(r) = V_V + V_S = -\frac{4\alpha_s}{3r} + Ar^\nu \quad (3)$$

as the static quark-antiquark interaction potential [14].

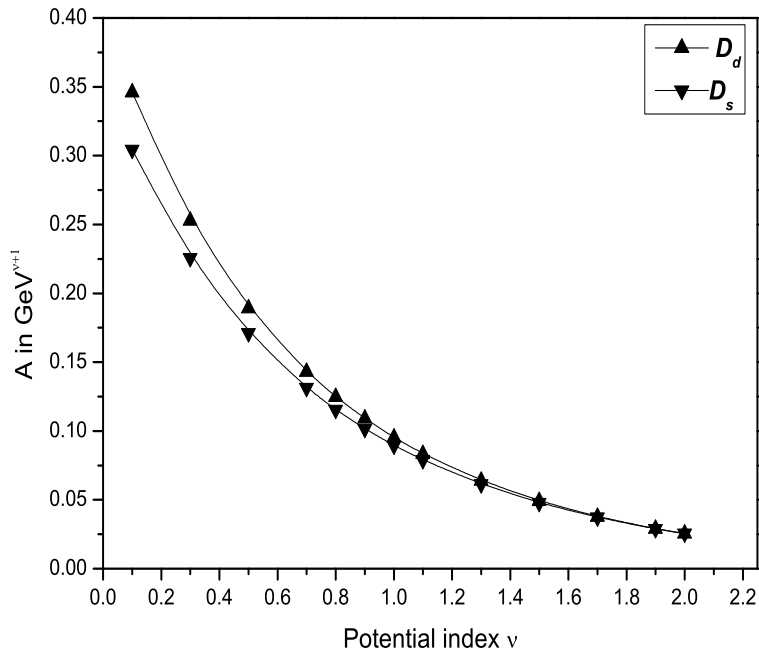


Figure 1: Behavior of  $A$  with the potential index  $\nu$  for  $D$  and  $D_s$  mesons.

## 2.1 Spin-dependent Forces

In general, the quark-antiquark bound states are represented by  $n^{2S+1}L_J$ , identified with the  $J^{PC}$  values, with  $\vec{J} = \vec{L} + \vec{S}$ ,  $\vec{S} = \vec{S}_q + \vec{S}_{\bar{q}}$ , parity  $P = (-1)^{L+1}$  and the charge conjugation  $C = (-1)^{L+S}$  with  $(n, L)$  being the radial quantum numbers. So the  $S$ -wave ( $L = 0$ ) bound states are represented by  $J^{PC} = 0^{-+}$  and  $1^{-+}$  respectively. The  $P$ -wave ( $L = 1$ ) states are represented by  $J^{PC} = 1^{+-}$  with  $L = 1$  and  $S = 0$  while  $J^{PC} = 0^{++}$ ,  $1^{++}$  and  $2^{++}$  correspond to  $L = 1$  and  $S = 1$  respectively. Thus, the spin-spin interaction among the constituent quarks provides the mass splitting of  $J = 0^{-+}$  and  $1^{-+}$  states, while the spin-orbit interaction provides the mass splitting of  $J^{PC} = 0^{++}$ ,  $1^{++}$  and  $2^{++}$  states. The  $J^{PC} = 1^{+-}$  state with  $L = 1$  and  $S = 0$  represents the spin average mass of the  $P$ -state as its spin-orbit contribution becomes zero, while the two  $J = 1^{+-}$  singlet and the  $J = 1^{++}$  of the triplet  $P$ -states can form a mixed state. The  $D$ -wave ( $L = 2$ ) states are represented by  $J^{PC} = 2^{-+}$  with  $L = 2$  and  $S = 0$  while  $J^{PC} = 3^{--}$ ,  $2^{--}$  and  $1^{--}$  correspond to  $L = 2$  and  $S = 1$  respectively. The  $F$ -wave ( $L = 3$ ) states are represented by  $J^{PC} = 3^{+-}$  with  $L = 3$  and  $S = 0$  while  $J^{PC} = 4^{++}$ ,  $3^{+-}$  and  $2^{++}$

correspond to  $L = 3$  and  $S = 1$  respectively.

For computing the mass difference between different degenerate meson states, we consider the spin dependent part of the usual one gluon exchange potential (OGEP) given by [27, 43, 44, 45, 46]. Accordingly, the spin-dependent part,  $V_{SD}(r)$  contains three components of the interaction terms, such as the spin-spin, the spin-orbit and the tensor part given by [44]

$$V_{SD}(r) = V_{SS}(r) \left[ S(S+1) - \frac{3}{2} \right] + V_{LS}(r) (\vec{L} \cdot \vec{S}) + V_T(r) \left[ S(S+1) - \frac{3(\vec{S} \cdot \vec{r})(\vec{S} \cdot \vec{r})}{r^2} \right] \quad (4)$$

The spin-orbit term containing  $V_{LS}(r)$  and the tensor term containing  $V_T(r)$  describe the fine structure of the meson states, while the spin-spin term containing  $V_{SS}(r)$  proportional to  $2(\vec{s}_q \cdot \vec{s}_{\bar{q}}) = S(S+1) - \frac{3}{2}$  gives the spin singlet-triplet hyperfine splitting.

The coefficient of these spin-dependent terms of Eqn.4 can be written in terms of the vector and scalar parts of the static potential,  $V_c(r)$  as [44]

$$V_{LS}(r) = \frac{1}{2 m_1 m_2 r} \left( 3 \frac{dV_V}{dr} - \frac{dV_S}{dr} \right) \quad (5)$$

$$V_T(r) = \frac{1}{6 m_1 m_2} \left( 3 \frac{d^2 V_V}{dr^2} - \frac{1}{r} \frac{dV_V}{dr} \right) \quad (6)$$

$$V_{SS}(r) = \frac{1}{3 m_1 m_2} \nabla^2 V_V = \frac{16 \pi \alpha_s}{9 m_1 m_2} \delta^{(3)}(\vec{r}) \quad (7)$$

The present study with the choices of  $\nu$  in the range  $0.1 < \nu < 2.0$ , is an attempt to know the predictability of the hadron spectroscopy with a chosen value of mass parameters ( $m_1, m_2$ ) and confinements strength represented by the potential parameter  $A$ . The running strong coupling constant appeared in the potential  $V(r)$  in turn is related to the quark mass parameter as

$$\alpha_s(\mu^2) = \frac{4\pi}{(11 - \frac{2}{3}n_f) \ln(\mu^2/\Lambda^2)} \quad (8)$$

Where,  $n_f$  is the number of flavors,  $\mu$  is renormalization scale related to the constituent quark masses as  $\mu = 2m_1 m_2 / (m_1 + m_2)$  and  $\Lambda$  is the QCD scale which is taken as 0.150 GeV by fixing  $\alpha_s = 0.118$  at the  $Z$ -boson mass (91 GeV)[47].

The potential parameter,  $A$  of Eqn.3 is similar to the string strength  $\sigma$  of the Cornell potential. The different choices of  $\nu$  here then correspond to different potential forms. So, the potential parameter  $A$  expressed in  $\text{GeV}^{\nu+1}$  can be different for each choices of  $\nu$ . The model potential

Table 1: Square of the radial wave functions at the origin( $|R_n(0)|^2$  (in  $\text{GeV}^3$ )) of  $Q\bar{q}$  systems in  $\text{CPP}_\nu$ .

Model	$D$			$D_s$		
	1S	2S	3S	1S	2S	3S
$\text{CPP}_\nu = 0.1$	0.050	0.011	0.005	0.063	0.014	0.007
0.3	0.083	0.028	0.016	0.104	0.034	0.020
0.5	0.111	0.047	0.031	0.139	0.058	0.038
0.7	0.135	0.068	0.049	0.168	0.084	0.061
0.8	0.145	0.079	0.060	0.181	0.098	0.074
0.9	0.155	0.091	0.071	0.193	0.112	0.088
1.0	0.164	0.102	0.083	0.204	0.127	0.103
1.1	0.172	0.114	0.096	0.214	0.142	0.118
1.3	0.186	0.139	0.123	0.232	0.172	0.153
1.5	0.199	0.164	0.154	0.247	0.203	0.190
2.0	0.222	0.227	0.237	0.276	0.280	0.292

parameter  $A$  and the mass parameter of the quark/antiquark ( $m_1, m_2$ ) are fixed using the known ground state center of weight (spin average) mass and the hyperfine splitting ( $M_{3S_1} - M_{1S_0}$ ) of  $D$  and  $D_s$  systems respectively. The spin average mass for the ground state is computed for the different choices of  $\nu$  in the range,  $0.1 \leq \nu \leq 2.0$ . The spin average or the center of weight mass,  $M_{CW}$  is calculated from the known experimental/theoretical values of the pseudoscalar ( $J = 0$ ) and vector ( $J = 1$ ) meson states as

$$M_{n,CW} = \frac{\sum_J (2J + 1) M_{nJ}}{\sum_J (2J + 1)} \quad (9)$$

## 2.2 Spectra of Heavy - Light Flavour ( $Q\bar{q}$ ) Mesons

The spectra of the heavy-light mesons are calculated using nonrelativistic hamiltonian as given by Eqn.1, where  $m_1 = m_Q$  and  $m_2 = m_{\bar{q}}$ . The spin average masses of  $D^* - D$  and the  $D_s^* - D_s$  mesons are computed using the experimental values of  $M_D = 1.869$  GeV,  $M_{D^*} = 2.010$  GeV,  $M_{D_s} = 1.968$  GeV,  $M_{D_s^*} = 2.112$  GeV respectively [47].

We employ the numerical approach as given by [48] to find the eigen values and radial wave functions of the respective Schrödinger equation. The potential parameter  $A$ , is made to vary

Table 2: The  $\ell^{th}$  derivative of orbitally excited radial wave functions at the origin ( $|R_n^\ell(0)|$  in  $\text{GeV}^{(\frac{3}{2}+\ell)}$ ) of  $Q\bar{q}$  systems in  $\text{CPP}_\nu$ .

Model	$D$				$D_s$			
	1P	2P	1D	1F	1P	2P	1D	1F
$\text{CPP}_\nu = 0.1$	0.0110	0.0083	0.0008	0.0001	0.0130	0.0097	0.0010	0.0001
0.3	0.0253	0.0210	0.0034	0.0006	0.0299	0.0253	0.0044	0.0008
0.5	0.0392	0.0358	0.0076	0.0018	0.0474	0.0428	0.0097	0.0024
0.7	0.0551	0.0520	0.0129	0.0040	0.0634	0.0619	0.0165	0.0055
0.8	0.0603	0.0604	0.0159	0.0055	0.0711	0.0722	0.0203	0.0076
0.9	0.0666	0.0692	0.0192	0.0073	0.0793	0.0826	0.0245	0.0103
1.0	0.0732	0.0780	0.0226	0.0093	0.0881	0.0931	0.0288	0.0126
1.1	0.0790	0.0870	0.0261	0.0115	0.0934	0.1029	0.0335	0.0157
1.3	0.0916	0.1043	0.0334	0.0166	0.1088	0.1243	0.0426	0.0227
1.5	0.1022	0.1221	0.0408	0.0225	0.1189	0.1459	0.0521	0.0307
2.0	0.1234	0.1653	0.0593	0.0397	0.1457	0.1969	0.0756	0.0542

with  $\nu$ , keeping the quark mass parameter fixed for each choices of  $Q\bar{q}$  system. It is observed that the hyperfine splitting of the  $1^3S_1$  and  $1^1S_0$  states are very sensitive to the choices of  $m_Q$  and  $A$ . The most suitable values of the quark mass parameter are found to be  $m_c = 1.28$  GeV,  $m_d = 0.35$  GeV  $m_s = 0.500$  GeV for our present study. The corresponding  $A$  values obtained from the  $1S$  fitting and are plotted in Fig.1 against the potential index  $\nu$  of the  $D$  and  $D_s$  systems. Just like the string tension  $\sigma(r)$  of the Cornell potential was made to vary for excited states [31, 32], we allow  $A$  to vary mildly with radial quantum number  $n$  as  $A \rightarrow \frac{A}{(n)^{\frac{1}{4}}}$  for computing the spin independent masses of the orbital excited ( $nL$ ) states. The variation in  $A$  can be justified by similar arguments for the changes in  $\alpha_s$  with the average kinetic energy. Here, as the system get excited, the average kinetic energy increases and hence the potential strength (the spring tension) reduces. With this mild state dependence on the potential parameter  $A$ , we obtain the spin average masses of the orbital excited states closer to the experimentally known  $D$  and  $D_s$  systems. The computed values of the radial wave function at the origin  $|R_{n\ell}^\ell(0)|$  for different states are listed in Table 1 ( $nS$ -states) and Table 2 ( $1P, 2P, 1D, 1F$ -states) for all the  $c\bar{q}$  ( $Q \in c$  and  $q \in u/d, s$ ) combinations. Using the spin dependent potential given by Eqn.4, we compute the masses of the different  $n^{2S+1}L_J$  low lying states of  $c\bar{q}$  and are listed in Table 3 and 4 in the case of  $D$  and  $D_s$  mesons respectively. The available experimental values as well as other model predictions are also listed for comparison.

Table 3: Mass spectra (in GeV) of  $D$  meson.

State	Potential index $\nu$										Expt.	RQM	RQM	BSU
	0.1	0.7	0.8	0.9	1.0	1.1	1.3	1.5	1.7	2.0	[47]	[26]	[2]	[49]
$1^3S_1$	1.985	2.007	2.010	2.013	2.015	2.018	2.021	2.025	2.028	2.031	2.010	2.009	2.005	2.006
$1^1S_0$	1.932	1.864	1.855	1.848	1.841	1.834	1.823	1.813	1.805	1.794	1.869	1.875	1.868	1.874
$1^3P_2$	2.070	2.268	2.294	2.319	2.342	2.364	2.404	2.440	2.472	2.514	2.460	2.459	2.460	2.477
$1^3P_1$	2.072	2.282	2.310	2.336	2.361	2.384	2.426	2.465	2.498	2.542		2.414	2.417	2.407
$1^3P_0$	2.068	2.261	2.287	2.312	2.335	2.357	2.398	2.434	2.467	2.510		2.438	2.490	2.341
$1^1P_1$	2.062	2.216	2.235	2.253	2.269	2.285	2.312	2.337	2.358	2.385		2.501	2.377	2.389
$2^3S_1$	2.011	2.303	2.350	2.398	2.445	2.491	2.582	2.668	2.751	2.868		2.629	2.692	2.601
$2^1S_0$	1.998	2.226	2.261	2.296	2.329	2.362	2.425	2.483	2.538	2.612		2.579	2.589	2.540
$1^3D_3$	2.106	2.456	2.508	2.558	2.605	2.651	2.736	2.816	2.887	2.984			2.799	2.688
$1^3D_2$	2.106	2.454	2.504	2.552	2.597	2.639	2.717	2.788	2.851	2.933			2.775	2.727
$1^3D_1$	2.105	2.459	2.512	2.564	2.613	2.661	2.751	2.836	2.913	3.019			2.833	2.750
$1^1D_2$	2.104	2.455	2.509	2.561	2.612	2.662	2.756	2.846	2.930	3.046			2.795	2.689
$2^3P_2$	2.037	2.432	2.499	2.565	2.631	2.696	2.824	2.949	3.069	3.241			3.035	2.860
$2^3P_1$	2.038	2.443	2.511	2.580	2.648	2.715	2.847	2.976	3.100	3.279			2.995	2.802
$2^3P_0$	2.036	2.427	2.493	2.559	2.624	2.689	2.816	2.940	3.059	3.231			3.045	2.758
$2^1P_1$	2.033	2.394	2.454	2.512	2.570	2.627	2.736	2.843	2.944	3.087			2.949	2.792
$3^3S_1$	2.005	2.468	2.553	2.640	2.727	2.816	2.994	3.172	3.348	3.607			3.226	2.947
$3^1S_0$	1.999	2.413	2.486	2.560	2.634	2.708	2.855	2.999	3.139	3.340			3.141	2.904
$1^3F_4$	2.127	2.607	2.683	2.757	2.829	2.900	3.033	3.159	3.276	3.436			3.091	
$1^3F_3$	2.127	2.599	2.671	2.741	2.807	2.871	2.989	3.096	3.192	3.318			3.074	
$1^3F_2$	2.127	2.611	2.688	2.764	2.839	2.911	3.051	3.184	3.308	3.481			3.123	
$1^1F_3$	2.127	2.617	2.698	2.778	2.857	2.936	3.089	3.238	3.382	3.587			3.101	

Relativistic Quark Model (RQM), Blankenbecler- Sugar Equation (BSU).



Table 4: Mass spectra (in GeV) of  $D_s$  meson.

State	Potential index $\nu$										Expt.	RQM	RQM	BSU
	0.1	0.7	0.8	0.9	1.0	1.1	1.3	1.5	1.7	2.0	[47]	[26]	[2]	[49]
$1^3S_1$	2.086	2.102	2.104	2.106	2.108	2.109	2.112	2.114	2.116	2.119	2.112	2.111	2.113	2.108
$1^1S_0$	2.047	1.998	1.992	1.987	1.982	1.977	1.969	1.962	1.956	1.948	1.968	1.981	1.965	1.975
$1^3P_2$	2.165	2.348	2.372	2.394	2.416	2.436	2.474	2.506	2.535	2.573	2.572	2.560	2.581	2.586
$1^3P_1$	2.162	2.332	2.355	2.376	2.397	2.416	2.452	2.484	2.512	2.549	2.535	2.515	2.535	2.522
$1^3P_0$	2.157	2.300	2.317	2.334	2.350	2.364	2.391	2.414	2.433	2.459	2.317	2.569	2.487	2.455
$1^1P_1$	2.163	2.337	2.360	2.382	2.402	2.422	2.457	2.488	2.516	2.552	2.460	2.508	2.605	2.502
$2^3S_1$	2.110	2.355	2.395	2.434	2.474	2.513	2.588	2.661	2.730	2.828		2.716	2.806	2.722
$2^1S_0$	2.101	2.303	2.334	2.365	2.395	2.425	2.482	2.535	2.585	2.654		2.670	2.700	2.659
$1^3D_3$	2.195	2.502	2.545	2.587	2.627	2.666	2.736	2.799	2.880	2.965			2.925	2.857
$1^3D_2$	2.195	2.505	2.551	2.595	2.639	2.681	2.760	2.832	2.855	2.929			2.900	2.856
$1^3D_1$	2.194	2.502	2.548	2.594	2.638	2.681	2.763	2.839	2.899	2.989			2.913	2.845
$1^1D_2$	2.195	2.503	2.548	2.591	2.633	2.674	2.749	2.818	2.909	3.007			2.953	2.838
$2^3P_2$	2.136	2.489	2.549	2.608	2.668	2.727	2.843	2.954	3.040	3.190			3.157	2.988
$2^3P_1$	2.134	2.478	2.535	2.593	2.651	2.708	2.820	2.928	3.062	3.217			3.114	2.942
$2^3P_0$	2.132	2.455	2.507	2.560	2.612	2.663	2.763	2.858	3.032	3.182			3.067	2.901
$2^1P_1$	2.135	2.482	2.540	2.598	2.656	2.713	2.826	2.935	2.949	3.078			3.165	2.928
$3^3S_1$	2.105	2.497	2.568	2.641	2.715	2.790	2.940	3.090	3.238	3.456			3.345	3.087
$3^1S_0$	2.101	2.459	2.523	2.587	2.652	2.717	2.846	2.973	3.096	3.275			3.259	3.044
$1^3F_4$	2.214	2.630	2.693	2.755	2.814	2.872	2.979	3.075	3.221	3.361			3.220	
$1^3F_3$	2.214	2.638	2.705	2.771	2.836	2.900	3.022	3.136	3.163	3.278			3.224	
$1^3F_2$	2.214	2.642	2.711	2.780	2.849	2.917	3.048	3.175	3.244	3.392			3.247	
$1^1F_3$	2.214	2.635	2.702	2.766	2.830	2.892	3.010	3.119	3.295	3.466			3.203	

Relativistic Quark Model (RQM), Blankenbecler- Sugar Equation (BSU).

### 3 The Decay constants of the charm flavored mesons

The decay constants of mesons are important parameters in the study of leptonic or non-leptonic weak decay processes. The decay constants of pseudoscalar ( $f_P$ ) and vector ( $f_V$ ) states are obtained by parameterizing the matrix elements of weak current between the corresponding mesons and the vacuum as [50]

$$\langle 0 | \bar{q} \gamma^\mu \gamma_5 c | P_\mu(k) \rangle = i f_P k^\mu \quad (10)$$

$$\langle 0 | \bar{q} \gamma^\mu c | V(k, \epsilon) \rangle = f_V M_V \epsilon^\mu \quad (11)$$

where  $k$  is the meson momentum,  $\epsilon^\mu$  and  $M_V$  are the polarization vector and mass of the vector meson.

In the relativistic quark model, the decay constant can be expressed through the meson wave function  $\Phi_{P/V}(p)$  in the momentum space [26].

$$f_{P/V} = \sqrt{\frac{12}{M_{P/V}}} \int \frac{d^3 p}{(2\pi)^3} \left( \frac{E_c(p) + m_c}{2E_c(p)} \right)^{1/2} \left( \frac{E_{\bar{q}}(p) + m_{\bar{q}}}{2E_{\bar{q}}(p)} \right)^{1/2} \left\{ 1 + \lambda_{P/V} \frac{p^2}{[E_c(p) + m_c][E_{\bar{q}}(p) + m_{\bar{q}}]} \right\} \Phi_{P/V}(p) \quad (12)$$

with  $\lambda_P = -1$  and  $\lambda_V = -1/3$ . In the nonrelativistic limit  $\frac{p^2}{m^2} \ll 1.0$ , this expression reduces to the well known relation between  $f_{P/V}$  and the ground state wave function at the origin  $R_{P/V}(0)$  the Van-Royen-Weisskopf formula [51]. Though most of the models predict the meson mass spectrum successfully, there exist wide range of predictions of their decay constants. For example, the ratio  $\frac{f_P}{f_V}$  was predicted to be  $> 1$  in most of the nonrelativistic cases, as  $m_P < m_V$  and their wave function at the origin has assumed to be as  $R_P(0) \sim R_V(0)$  [52]. The ratio computed in the relativistic models [53] have predicted  $\frac{f_P}{f_V} < 1$ , particularly in the  $Q\bar{Q}$  sector, but  $\frac{f_P}{f_V} > 1$  in the heavy-light flavour sector. The disparity of the predictions of these decay constants play decisive role in the precision measurements of the weak decay parameters. The value of the radial wave function ( $R_P$ ) for  $0^{-+}$  and ( $R_V$ ) for  $1^{--}$  states would be different due to their spin dependent hyperfine interaction. The spin hyperfine interaction of the heavy flavour mesons are small and this can cause a small shift in the value of the wave function at the origin. Though, many models neglect this difference between ( $R_P$ ) and ( $R_V$ ), we consider this correction by making an ansatz that the  $R_{P/V}(0)$  are related to the value of the radial wave function at the origin,  $R_n(0)$  according to the same way their masses are related. Thus, by considering

$$M_{nP/V} = M_{n,CW} \left[ 1 + (SF)_{P/V} \frac{\langle V_{SS} \rangle_n}{M_{n,CW}} \right] \quad (13)$$

Table 5: The decay constants  $f_{P/V}$  in MeV of  $D$  and  $D_s$  systems (The bracketed quantities are with QCD correction).

		$D$			$D_s$		
Models		1S	2S	3S	1S	2S	3S
$f_P$	CPP $_{\nu}$ =0.1	154(120)	73(57)	51(40)	169(131)	80(62)	55(43)
	0.3	197(155)	111(88)	85(67)	216(167)	122(95)	93(72)
	0.5	227(178)	141(111)	113(89)	249(193)	155(120)	124(96)
	0.7	248(195)	166(131)	137(108)	273(211)	184(142)	152(118)
	0.8	257(202)	177(139)	148(117)	283(219)	196(152)	165(128)
	0.9	265(208)	188(148)	159(125)	291(226)	208(161)	177(137)
	1.0	272(213)	197(155)	169(133)	299(232)	219(170)	189(146)
	1.1	278(218)	207(162)	178(140)	306(237)	230(178)	200(155)
	1.3	289(226)	223(175)	196(154)	318(246)	249(193)	221(171)
	1.5	297(233)	238(187)	212(167)	327(254)	267(207)	240(186)
	RQM[54]	234			268		
	BS[55, 53]	230 $\pm$ 25			248 $\pm$ 27		
		$D^*$			$D_s^*$		
$f_V$	CPP $_{\nu}$ =0.1	156(104)	73(49)	51(34)	170(116)	80(54)	55(38)
	0.3	202(135)	112(75)	85(57)	219(149)	123(84)	93(63)
	0.5	234(157)	143(96)	114(76)	254(173)	157(107)	125(85)
	0.7	258(173)	169(113)	139(93)	280(190)	186(126)	153(104)
	0.8	268(180)	181(121)	150(101)	290(198)	199(135)	166(113)
	0.9	277(186)	192(128)	161(108)	300(204)	211(144)	179(122)
	1.0	285(191)	202(135)	172(115)	308(210)	223(152)	191(130)
	1.1	292(196)	212(142)	182(122)	316(215)	234(159)	203(138)
	1.3	304(204)	230(154)	201(134)	329(224)	255(173)	224(153)
	1.5	314(211)	247(165)	218(146)	340(231)	273(186)	244(166)
	RQM[54]	310			315		
	BS[55, 53]	340 $\pm$ 23			375 $\pm$ 24		

Table 6: Pseudoscalar  $f_P$  decay constants for  $D$  mesons in (MeV)

	$f_P(D)$		$f_P(D_s)$		$f_P(D_s)/f_P(D)$	
	Our	Others	Our	Others	Our	Others
CPP $_{\nu=0.1}$	154(120)		169(131)		1.097(1.084)	
0.3	197(155)	230[59]	216(167)	248[59]	1.096(1.082)	1.08[59]
0.5	227(178)	234[54]	249(193)	268[54]	1.096(1.083)	1.15 [54]
0.7	248(195)	203[60]	273(211)	235[60]	1.098(1.084)	1.15[60]
0.8	257(202)	208[61]	283(219)	241[61]	1.098(1.084)	1.164[61]
0.9	265(208)	201[62]	291(226)	249[62]	1.098(1.085)	1.24[62]
1.0	272(213)	206[63]	299(232)	220[63]	1.099(1.086)	1.07[63]
1.1	278(218)	235[64]	306(237)	266[64]	1.099(1.086)	1.13[64]
1.3	289(226)	223[65]	318(246)	276[65]	1.101(1.087)	1.23[65]
1.5	297(233)		327(254)		1.101(1.088)	

and following the fact that any  $c$ -number,  $a$ , commutes with the Hamiltonian, *i.e.*  $aH\Psi = H(a\Psi)$ , we express,

$$R_{nP/V}(0) = R_n(0) \left[ 1 + (SF)_{P/V} \frac{(M_{nV} - M_{nP})}{M_{n,CW}} \right] \quad (14)$$

Here  $(SF)_P = -\frac{3}{4}$  and  $(SF)_V = \frac{1}{4}$  are the spin factor corresponding to the pseudoscalar ( $J = 0$ ) spin coupling and vector ( $J = 1$ ) spin coupling respectively [40].  $M_{n,CW}$  and  $R_n(0)$  are spin average mass and the normalized spin independent wave function at the origin of the meson state respectively. It can easily be seen that this expression given by Eqn 14 is consistent with the relation

$$R(0) = \frac{3R_V(0) + R_P(0)}{4} \quad (15)$$

given by [14, 56] for  $nS$  states. The decay constants by incorporating first order QCD correction to the Van Royen-Weiskopff formula are given by [57, 58],

$$f_{P/V}^2(nS) = \frac{3 |R_{nP/V}(0)|^2}{\pi M_{nP/V}} \bar{C}^2(\alpha_s) \quad (16)$$

where, the first order QCD correction factor,  $\bar{C}(\alpha_s)$  is expressed for the  $Q\bar{q}$  system as

$$\bar{C}(\alpha_s) = 1 + \frac{\alpha_s}{\pi} \left[ \frac{m_1 - m_2}{m_1 + m_2} \ln \frac{m_1}{m_2} - \delta^{V,P} \right] \quad (17)$$

Here  $\delta^V = \frac{8}{3}$  [57, 66] and  $\delta^P = 2$  [57, 58, 66]. For the  $Q\bar{q}$  system,  $m_1 = m_Q$  and  $m_2 = m_{\bar{q}}$ . We re-examine the predictions of the decay constants  $f_P$  and  $f_V$  under different potential schemes (by the choices of different  $\nu$ ) with and without the QCD correction. Our computed results up to  $3S$  states of the  $D$  and  $D_s$  systems are tabulated in Tables 5. The ratio of  $\frac{f_P(D_s)}{f_P(D)}$  for  $1S$  state

Table 7: The root mean square radii (in  $fm$ ) of  $D$  and  $D_s$  systems.

State	Model	1S	2S	3S	1P	2P	1D	1F
$D$	CPP $_{\nu}$ = 0.1	1.344	3.991	7.202	3.000	6.124	4.647	6.262
	0.3	1.043	2.687	4.429	1.966	3.702	2.799	3.587
	0.5	0.903	2.136	3.347	1.567	2.800	2.140	2.669
	0.7	0.818	1.813	2.734	1.343	2.300	1.781	2.178
	0.8	0.787	1.696	2.515	1.263	2.124	1.656	2.008
	0.9	0.761	1.597	2.334	1.198	1.978	1.553	1.869
	1.0	0.738	1.514	2.182	1.143	1.856	1.467	1.754
	1.1	0.719	1.442	2.051	1.095	1.752	1.394	1.657
	1.3	0.687	1.323	1.840	1.019	1.584	1.278	1.502
	1.5	0.663	1.231	1.678	0.961	1.455	1.189	1.385
$D_s$	CPP $_{\nu}$ = 0.1	1.255	3.749	6.777	2.819	5.780	4.381	5.914
	0.3	0.979	2.532	4.182	1.855	3.500	2.646	3.395
	0.5	0.848	2.015	3.161	1.479	2.646	2.023	2.524
	0.7	0.769	1.710	2.581	1.267	2.172	1.682	2.058
	0.8	0.740	1.599	2.374	1.192	2.005	1.564	1.897
	0.9	0.715	1.506	2.203	1.130	1.867	1.466	1.766
	1.0	0.694	1.427	2.058	1.077	1.751	1.385	1.656
	1.1	0.676	1.359	1.935	1.033	1.652	1.315	1.564
	1.3	0.646	1.247	1.735	0.960	1.493	1.205	1.417
	1.5	0.623	1.159	1.581	0.905	1.371	1.120	1.305

is tabulated against different choices of  $\nu$  in Table 6. The present results are in accordance with other predictions as seen from the the pseudoscalar decay constant  $f_D$  and  $f_{D_s}$ .

## 4 Root mean square Radii of the $D$ and $D_s$ meson states and Average quark Velocities

The mean square size of the meson is an important parameter in the estimations of hadronic transition widths [67, 71, 72], while the average velocity of the quarks within a quark-antiquark bound state is important for the estimation of the relativistic corrections and useful particularly in the NRQCD formalism. It is also important in the estimation of their production rates [73].

Table 8: Mean square velocity of the quark within  $D$  and  $D_s$  states.

State	Model	1S	2S	3S	1P	2P	1D	1F
$D$	CPP $_{\nu} = 0.1$	0.197	0.091	0.066	0.098	0.069	0.077	0.069
	0.3	0.307	0.208	0.184	0.220	0.190	0.208	0.208
	0.5	0.397	0.334	0.331	0.341	0.332	0.353	0.372
	0.7	0.472	0.469	0.504	0.459	0.492	0.506	0.556
	0.8	0.506	0.539	0.599	0.517	0.578	0.584	0.653
	0.9	0.537	0.610	0.700	0.573	0.666	0.662	0.753
	1.0	0.566	0.681	0.805	0.628	0.757	0.740	0.853
	1.1	0.593	0.754	0.914	0.681	0.850	0.818	0.955
	1.3	0.642	0.899	1.142	0.783	1.041	0.971	1.160
	1.5	0.685	1.043	1.381	0.878	1.234	1.120	1.363
$D_s$	CPP $_{\nu} = 0.1$	0.133	0.060	0.043	0.065	0.046	0.051	0.045
	0.3	0.205	0.136	0.121	0.145	0.124	0.136	0.135
	0.5	0.263	0.219	0.217	0.224	0.217	0.231	0.243
	0.7	0.313	0.308	0.330	0.302	0.323	0.331	0.364
	0.8	0.335	0.354	0.393	0.340	0.379	0.383	0.428
	0.9	0.355	0.401	0.459	0.377	0.437	0.434	0.493
	1.0	0.375	0.448	0.528	0.413	0.497	0.486	0.560
	1.1	0.393	0.496	0.600	0.448	0.559	0.537	0.627
	1.3	0.425	0.592	0.751	0.516	0.684	0.639	0.762
	1.5	0.454	0.687	0.909	0.579	0.812	0.737	0.897

Thus with our numerical radial wave functions obtained for different choices of the potential index  $\nu$ , we compute the mean square radii of the meson state as

$$\langle r^2 \rangle_{nl} = \int_0^\infty r^4 |R_{nl}(r)|^2 dr \quad (18)$$

and the average mean square velocity of the quark/antiquark inside the state as [74]

$$\left\langle \frac{v^2}{c^2} \right\rangle_{nl} = \frac{1}{2M_1} (E_{nl} - \langle V(r) \rangle_{nl}) \quad (19)$$

Here,  $E_{nl}$  is the binding energy of the  $n^{\ell^{th}}$  state and  $\langle V(r) \rangle_{nl}$  is the expectation value of the quark-antiquark interaction (without spin dependent terms) potential energy in that state. The computed root mean square radii and the relative mean square velocities of the bound states within the mesons are tabulated in Table 7 and Table 8 with different choices of  $\nu$  respectively.

## 5 Inclusive Semileptonic Decay of Open Charm Flavour Mesons

Inclusive widths of the heavy flavor hadrons are examples of the genuine short-distance processes. The open charm mesons, decay through,  $c \rightarrow q\ell^+\nu$ , where  $q = d, s$ . The light  $d$  or  $s$  daughter quark is bound to the initial light quark of the charm meson by the strong interaction to form a new hadron  $X$ , according to the Feynman diagram of Fig.2.

In semileptonic decays, the two leptons do not feel the strong interaction, and are thus free of strong binding effects. Therefore, they can be factored out of the hadronic matrix element in the amplitude of the semileptonic decay process as

$$A = \frac{G_F}{\sqrt{2}} V_{cq}^* \bar{\nu} \gamma_\mu (1 - \gamma_5) l \langle X | \bar{q} \gamma^\mu (1 - \gamma_5) c | D \rangle, \quad (20)$$

where all strong interactions are included in the hadronic matrix element  $\langle X | \bar{q} \gamma^\mu (1 - \gamma_5) c | D \rangle$ . The amplitude of the semileptonic decay process depends both on the hadronic matrix element and the quark-mixing parameter  $V_{cq}$ —the Cabibbo-Kobayashi-Maskawa (CKM) matrix element. Thus, the semileptonic charm meson decay process is a good laboratory for both studying the quark-mixing mechanism and testing theoretical techniques developed for calculating the hadronic matrix element. The hadronic matrix element can be decomposed into several form factors according to its Lorentz structure. The form factors are generally controlled by non-perturbative dynamics, since perturbative QCD could not be applied directly.

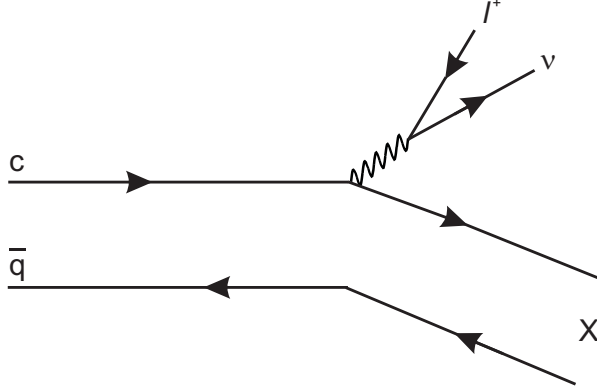


Figure 2: Feynman diagram for semileptonic  $D$  Decay

For the present study, we compute the decay width of the  $D$  and  $D_s$  mesons using the nonperturbative bound state effects. The decay width and branching ratio for the  $\Gamma(D \rightarrow \bar{K}^0 + e^+ + \nu_e)$  and  $\Gamma(D_s \rightarrow \phi + \ell^+ + \nu_\ell)$  mesons are calculated using the expression given by [68, 69, 70],

$$\Gamma_{sl}(D) = \frac{G_F^2 m_c^5}{192\pi^3} (|V_{cs}|^2 + |V_{cd}|^2) \left[ f(x) - \frac{\alpha_s}{\pi} g(x) \right] \quad (21)$$

$$\Gamma_{sl}(D_s) = \frac{G_F^2 m_c^5}{192\pi^3} |V_{cs}|^2 \left[ f(x) - \frac{\alpha_s}{\pi} g(x) \right] \quad (22)$$

where  $f(x) = 1 - 8x + 8x^3 - x^4 - 12x^2 \log x$ , and the analytic expression of the function  $g(x)$  is given by [50, 68]

$$g(x) = -15.28x^6 + 48.68x^5 - 60.06x^4 + 35.3x^3 - 8.11x^2 - 1.97x + 2.41 \quad (23)$$

Here, the parameter  $x$  is computed as  $x = m_s^2 / (m_c^{eff})^2$ . Generally, for the calculation of the semileptonic decay of the heavy flavour mesons, the  $m_s$  is taken as the model mass parameters coming from the fitting of its mass spectrum. However, taking into account of the binding energy effects of the decaying heavy quark within the potential confinement scheme, we consider the decaying heavy quark mass as the effective mass of the quarks,  $m_q^{eff}$ . Accordingly, we define the effective masses of the quarks in the  $Q\bar{q}$  system as

$$\begin{aligned} m_Q^{eff} &= m_Q \left( 1 + \frac{\langle E_{bind} \rangle}{m_Q + m_{\bar{q}}} \right) \\ m_{\bar{q}}^{eff} &= m_{\bar{q}} \left( 1 + \frac{\langle E_{bind} \rangle}{m_Q + m_{\bar{q}}} \right) \end{aligned} \quad (24)$$

to account for its bound state effects. The binding effect has been calculated as  $\langle E_{bind} \rangle = M_{Q\bar{q}} - (m_Q + m_{\bar{q}})$ , where  $m_Q$  and  $m_{\bar{q}}$  are the model mass parameters employed in its spectroscopic



Table 9: The inclusive semileptonic BR of  $D \rightarrow \bar{K}^0 + e^+ + \nu_e$  and  $D_s \rightarrow \phi + \ell^+ + \nu_\ell$  states in %.

CPP $_\nu \rightarrow$	0.1	0.3	0.5	0.7	0.8	0.9	1.0	1.1	1.3	1.5	Expt.[47]
BR $_D$	7.4	6.7	6.1	5.6	5.4	5.3	5.1	5.0	4.7	4.5	8.6 $\pm$ 0.5
BR $_{D_s}$	2.77	2.57	2.42	2.29	2.24	2.19	2.15	2.11	2.04	1.98	2.36 $\pm$ 0.26

study and  $M_{Q\bar{q}}$  is the mass of the mesonic state. The effective mass of the quarks would be different from the adhoc choices of the model mass parameters. For example, within the meson the mass of the quarks may get modified due to its binding interactions with other quark. Thus, the effective mass of the charm quark will be different when it is in  $c\bar{s}$  combinations or in  $c\bar{d}$  combinations due to the residual strong interaction effects of the bound systems.

From the computed inclusive semileptonic decay widths, the Branching ratio of  $D_q$  mesons are taken here from the relation

$$BR = \Gamma_{sl} \times \tau, \quad (25)$$

The Lifetime of these mesons ( $\tau_D = 1.04 \text{ ps}^{-1}$  and  $\tau_{D_s} = 0.5 \text{ ps}^{-1}$ ) are obtained from the world average value reported by Particle Data Group (PDG-2008)[47]. The computed results of  $D$  and  $D_s$  mesons are listed in Table: 9. Our results are found to be in agreement with experimental results at lower potential indexes  $\nu \approx 0.1$  to 0.5, which is consistent with the agreement observed for their spectroscopy.

## 6 Leptonic Decay of the Open Heavy Flavour Mesons

Charged mesons formed from a quark and anti-quark can decay to a charged lepton pair when these objects annihilate via a virtual  $W^\pm$  boson (See Fig.3). quark-antiquark annihilations

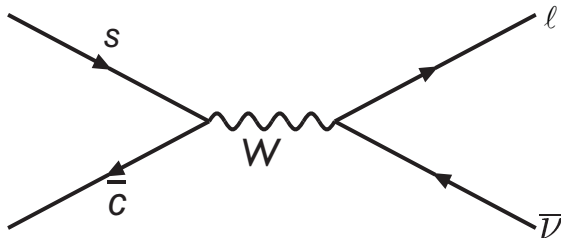


Figure 3: Feynman diagram in standard model for  $D_s \rightarrow \ell \bar{\nu}$  decay.

via a virtual  $W^+(W^-)$  to the  $\ell^+\nu(\ell^-\bar{\nu})$  final states occur for the  $\pi^\pm, K^\pm, D_s^\pm$  and  $B^\pm$  mesons. There are several reasons for studying the purely leptonic decays of charged mesons [65]. Such processes are rare but they have clear experimental signatures due to the presence of a highly energetic lepton in the final state. The theoretical predications are very clean due to the absence of hadrons in the final state [75]. The total leptonic width of  $D, D_s$  mesons are given by

$$\Gamma(D_q^+ \rightarrow \ell^+\nu_\ell) = \frac{G_F^2}{8\pi} f_{D_q}^2 |V_{cq}|^2 m_\ell^2 \left(1 - \frac{m_\ell^2}{M_{D_q}^2}\right)^2 M_{D_q}, \quad q = d, s \quad (26)$$

These transitions are helicity suppressed ; *i.e.*, the amplitude is proportional to  $m_\ell$ , the mass of the lepton  $\ell$ , in complete analogy to  $\pi^+ \rightarrow \ell^+\nu$ .

The leptonic widths of the charged  $D$  and  $D_s$  ( $1^1S_0$  state) mesons are obtained using Eqn.26 employing the predicted values of the pseudoscalar decay constants  $f_D$  and  $f_{D_s}$  along with the masses of the  $M_D$  and  $M_{D_s}$  obtained from the CPP $_\nu$  model. The leptonic widths for separate lepton channel by the choice of  $m_{\ell=\tau,\mu,e}$  are computed. The branching ratios of the total leptonic widths are then calculated using Eqn. 25. The present results as tabulated in Table 10 are in accordance with the available experimental values.

## 7 Result and Discussions

The spectroscopic results obtained for open charm ( $D, D_s$ ) mesons with different choice of the confining potential index  $\nu$  from 0.1 to 2.0 are tabulated along with other relativistic quark model predictions and with the known experimental states. Our predicted masses of  $P$ -wave  $D$ -meson state  $1^3P_2(2342 - 2514 \text{ MeV})$ ,  $1^3P_1(2361 - 2542 \text{ MeV})$ ,  $1^3P_0(2335 - 2510 \text{ MeV})$  and  $1^1P_1(2269 - 2385 \text{ MeV})$  for the choices of  $\nu$ ,  $1.0 \leq \nu \leq 2.0$  are in a accordance with other theoretical model prediction [2, 26, 49]. Similar agreement for the predicted masses for the  $2S, 1D, 2P, 3S$  and  $1F$  states are also observed in the same range of  $\nu$  values. While the experimental candidate for  $J^P = 2^+ D_1^*(2460)$ ,  $J^P = 1^+ D(2420)$  [47] and  $J^P = 0^+$  state observed in the range 2300 - 2400 MeV by Belle and Focus [76] lie within our predicted range. In the case of open strange-charm mesons ( $D_s$ ), our predictions within the range of  $\nu$ ,  $1.5 \leq \nu \leq 2.0$  for the  $1P, 2S, 1D, 2P, 3S$  and  $1F$  states of the  $D_s$  mesons are in accordance with other theoretical model prediction [2, 26, 49]. In particular the experimental states of  $D_{s2}(2573)$  [47] lie within our predicted range of  $1^3P_2$  (2416-2573),  $D_{s1}$  (2460) [47] lies in the predicted range of  $1^3P_1$  (2397-2549 MeV) for  $1.0 \leq \nu \leq 2.0$  and the  $D_{s0}^*$  (2317) [47] lies close to the predicted range of  $1^3P_0$  (2317-2350 MeV) for  $0.8 \leq \nu \leq 1.0$  of the CPP $_\nu$  model. The radial excitation of  $D_s^*(2715)$  by the Belle group[77] is found to be close to the predicted  $3^3S_1$  state for  $\nu = 1.0$ . Even higher excited states of  $c\bar{s}$  system has been observed by the BaBar collaboration [78] with spin parity  $0^+, 1^+$  and  $2^+$  *etc.*, with

mass at  $2856 \pm 1.5 \pm 5.0$  which in our case corresponds to the  $2P$  state with the predicted mass range of  $2^3P_2(2668 - 2954 \text{ MeV})$ ,  $2^3P_1(2651 - 2928 \text{ MeV})$ ,  $2^3P_0(2612 - 2858 \text{ MeV})$  and  $2^1P_1(2656 - 2935 \text{ MeV})$  with the choices of  $\nu$  in the range  $1.0 \leq \nu \leq 1.5$ . Thus the present study on the open charm and open strange-charm mesons using  $CPP_\nu$  model, we have been able to identify the recently discovered  $D$ -meson states as well as the  $D_s$ -meson states. Other predicted high angular momentum states  $\ell \geq 2$  of these mesons are expected to be seen in the future experiments at BES-III, BaBar, Belle and CLEO collaborations. Our  $1F$ - state mass predictions are in accordance with the theoretical predictions based on a relative quark model [2] but at higher choice of  $\nu$  ( $\nu \geq 1.5$ ).

Our results for  $f_P$  and  $f_V$  in the potential index ranging from 0.5 to 1.5 are fairly close to the known theoretical prediction as seen from Tables 5. The present tabulated results with QCD corrections (shown in brackets) are in agreement with the experimental values but higher potential index beyond  $\nu = 1.0$ . CLEO has reported the first significant measurement of  $f_{D^+} = 222.6 \pm 16.7 \text{ MeV}$  [79] which is close to our predicted value of 227 MeV (without QCD corrections) for  $\nu = 0.5$  and that 226 MeV (with QCD corrections) obtained at  $\nu = 1.3$ . The accuracy of the previous world average has been improved by BaBar with  $f_{D_s} = 283 \pm 17 \text{ MeV}$  [80] which within the range of values 273 - 283 MeV predicted here for the potential index  $0.7 \leq \nu \leq 0.8$  without QCD correction and goes beyond  $\nu = 1.5$  with QCD correction. However the ratio  $f_P(D_s(1S))/f_P(D(1S))$  is very close to each other between 1.09 to 1.10 (without the QCD correction) and between 1.082-1.088 (with QCD correction) with changing  $\nu$  from 0.1 to 1.5. The ratio predicted by the  $CPP_\nu$  model is thus very close to the ratio predicted by [59] and [63] but is lower than the ratio of 1.27 as per the recent experimental values of CLEO [79] and BaBar [80].

The semileptonic branching ratios of  $D$  and  $D_s$  mesons computed here using  $CPP_\nu$  model (See Table 9) are all found to be in good agreement with their respective experimental results. It can also be seen that the results do not vary appreciably with change in potential index  $\nu$ , indicating lesser influence of strong interaction effects in these decays. Though our predictions for  $D_s$  are well within the experimental error bar, the branching ratio of  $D$ -meson is slightly underestimated.

Present study on the leptonic decay branching ratios of  $D$  and  $D_s$  system presented in Table 10 are as per the available experimental limits. The branching ratio in  $\tau$ -lepton channel for  $D$  and  $D_s$  mesons lie within the predicted range for the potential index  $\nu \approx 0.3$  to 0.5. In the case of  $\mu$ -lepton channel, the experimental value of  $(4.4 \pm 0.7) \times 10^{-4}$  for  $D$ -meson lie in the predicted range for the potential index  $\nu = 0.3$  to 0.5 and that for  $D_s$  meson in the potential index  $\nu = 0.7$  to 0.8. Large experimental uncertainty in the electron channel make it difficult for any reasonable conclusion. Probably, future high luminosity better statistics and high confidence level data sets will be able to provide more light on the spectroscopy and decay properties of these open charm mesons.

**Acknowledgement:** Part of this work is done with a financial support from DST, Government of India, under a Major Research Project **SR/S2/HEP-20/2006**.

## References

- [1] Godfrey S and Kokoski R, Phys. Rev. **D43**, 1679 (1991).
- [2] M. Di Pierro *et al.*, Phys. Rev. **D64**, 114004 (2001).
- [3] Ebert D, Faustov R N and Galkin V O, Phys. Rev. **D57**, 014027 (1998).
- [4] Bardeen W A, Eichen E J and Hill C T, Phys. Rev. **D68**, 054024 (2003).
- [5] Colangelo P, Fazio F De and Ferrandes R, Nucl. Phys. (Proc. Suppl.)**D163**, 177 (2007).
- [6] Falk A F and Mehen T, Phys. Rev.**D53**, 231 (1996).
- [7] Eichen E J, Hill C T and Quigg C, Phys. Rev. Lett.**71**, 4116 (1993).
- [8] BaBar Collaboration, Aubert B *et al.*, Phys. Rev. Lett. **90**, 242001 (2003).
- [9] CLEO Collaboration, Besson D *et al.*, Phys. Rev. D **68**, 032002 (2003).
- [10] Belle Collaboration, Mikani Y *et al.*, Phys. Rev. Lett. **92**, 012002 (2004).
- [11] Godfrey S and Kokoski R, Phys. Rev. D **43**, 1679 (1991). Ebert D , Galkin V O, and Faustov R N, Phys. Rev. D **57**, 5663 (1998). Pierro M Di and Eichten E, Phys. Rev. D **64**, 114004 (2001). Lucha W and Schöberl F, Mod. Phys. Lett A **18**, 2837 (2003). Godfrey S, J. Phys. Conf. Ser. **9**, 59 (2005).
- [12] Brambilla N , in Proceedings of the VIII<sup>th</sup> International Workshop on Heavy Quarks and Leptons (HQL06), Munich (2006), edited by S.Recksiegel et al., eConf C0610161, 51 (2007) [hep-ph/0702105v2].
- [13] Brambilla N, Sumino Y and Vairo A, Phys. Rev. **D65**, 034001 (2002).
- [14] Rai A K, Patel B and Vinodkumar P C, Phys. Rev. **C78**, 055202 (2008).
- [15] Rai A K, Pandya J N and Vinodkumar P C, Eur. Phys. J. **A4**, 77 (2008).
- [16] Pandya J N and Vinodkumar P C, Pramana J. Phys **57**, 821 (2001).

- [17] Radford S F and Repko W W, Phys. Rev. **D75**, 074031 (2007).
- [18] Buchmüller and Tye, Phys. Rev. **D24**, 132 (1981).
- [19] Martin A, Phys. Lett. **B93**, 338 (1980).
- [20] Martin A, Phys. Lett. **B82**, 272 (1979).
- [21] Quigg C and Rosner J L, Phys. Lett. **B71**, 153 (1977).
- [22] Quigg C and Rosner J L, Phys. Rep. **56**, 167 (1979).
- [23] Eichten E *et al.*, Phys. Rev. **D17**, 3090 (1978).
- [24] VijayaKumar K B, Hanumaiah B and Pepin S, Eur.Phys. J. **A19**, 247 (2004).
- [25] Altarelli G, Cabibbo N, Corbo G, Maiani L and Martinelli G, Nucl. Phys. **B208**, 365 (1982).
- [26] Ebert D, Faustov R N and Galkin V O, Phys. Rev. **D67**, 014027 (2003).
- [27] Lakhina O and Swanson E S, Phys. Rev. **D74**, 014012 (2006).
- [28] Choi H M, Phys. Rev. **D75**, 073016 (2007).
- [29] Bali G S *et al.*, Phys. Rev **D62**, 054503 (2000); Bali G S, Phys. Rep. **343**, 1 (2001).
- [30] Alexandrou C , P de Forcrand and John O, Nucl. Phys. Proc. Suppl **119**, 667 (2003).
- [31] Badalian A M , Bakker B L G and Simonov Yu A, Phys. Rev. **D66**, 034026 (2002).
- [32] Badalian A M , Bakker B L G and Danilkin I V , arXiv:hep-ph/0805.2291.v1.
- [33] Albertus C *et al.*, Phys. Rev. **D71**, 113006 (2005).
- [34] M. Fabre de la Ripelle , Phys. Lett. **B205**,97 (1988).
- [35] Ebert D, Faustov R N and Galkin V O, Mod. Phys. Lett **A18** 601-608 (2003).
- [36] Lansberg J P and Pham T N, Phys. Rev. D **74**, 034001 (2006) , Phys. Rev. **D75**, 017501 (2007), arXiv:hep-ph/0804.2180v1.
- [37] Kim C S, Lee T and Wang G L, Phys. Lett. **B606**, 323(2005),arXiv:hep-ph/0411075.
- [38] Rosner J L et al. (CLEO Collaboration), Phys. Rev. Lett. **96**, 092003 (2006).
- [39] Rai A K (PhD Thesis), Sardar Patel University (2005)

- [40] Patel B and Vinodkumar P C, J. Phy. G : Nucl Part. Phy. **36**, 035003 (2009).
- [41] Rai A K, Parmar R H and Vinodkumar P C, J. Phys. G: Nucl. Part. Phys. **28**, 2275(2002).
- [42] Rai A K and Vinodkumar P C, Pramana J. Phys. **66**, 953 (2006).
- [43] Branes T, Godfrey S and Swanson E S, Phys.Rev. **D72**, 054026 (2005).
- [44] Voloshin M B, Prog. Part. Nucl. Phys. **61**, 455 (2008);arXiv:hep-ph/0711.4556v3.
- [45] Eichten E, Godfrey S, Mahlke H and Rosner J L, Rev. Mod. Phys. **80**, 1161 (2008).
- [46] Gershtein S S, Kiselev V V, Likhoded A K and Tkabladze A V, Phys. Rev. **D51**, 3613 (1995).
- [47] Amsler C *et al.* (Particle Data Group), Phys. Lett. **B**, 1 (2008)
- [48] Lucha W and Schöberl F, Int. J. Mod. Phys. **C10**, 607 (1999), arXiv:hep-ph/9811453v2.
- [49] T A Lähde, C J Nyfält and D O Riska, Nucl. Phys.**A674**, 141 (2000).
- [50] Quang Ho-Kim and Pham Xuan-Yem, “The particles and their interactions: Concept and Phenomena” Springer-Verlag (1998).
- [51] Van Royen R and Weisskopf V F, Nuovo Cimento **50**, (1967).
- [52] Hwang D S and Gwang-Hee Kim, Z. Phys. **C76**, 107 (1997).
- [53] Wang G L, Phys. Lett. **B633**, 492 (2006).
- [54] Ebert D *et al.*, Phys. Lett. **B634**, 214 (2006).
- [55] Cvetic G *et al.*, Phys. Lett. **B596**, 84 (2004).
- [56] Bodwin G T, Lee J and Sinclair D K, Phys. Rev. **D51**, 1125 (1995).
- [57] Berezhnoy A V, Kiselev V V and Likhoded A K, Z. Physik **A336**, 89 (1996).
- [58] Braaten E and Fleming S, Phys. Rev. **D52**, 181 (1995).
- [59] Gvetic G *et al.*, Phys. Lett**B596**, 84 (2004).
- [60] Narison S, Phys. Rev. Lett.**B520**, 115 (2001).
- [61] Follana E *et al.*, (HPQCD and UKQCD Collabs.), [arXiv:0706.1726](2007).
- [62] Aubin C *et al.*, Phys. Rev. Lett.**95**, 122002 (2005).

- [63] Khan A A *et al.*, (QCDSF Collaboration), Phys. Lett. **B652**, 150 (2007).
- [64] Chiu T W *et al.*, Phys. Lett. **B624**, 31 (2005).
- [65] Rosner J L and Stone S, arXiv:hep-ex/0802.1043v1.
- [66] Gerstein S S *et al.*, arXiv:hep-ph/9803433v1.
- [67] Gottfried K, Phys. Rev. Lett. **40**, 598 (1978).
- [68] Yosef NIR, Phys. Lett. **B221**, 184 (1989).
- [69] N Cabibbo *et al.*, Phys. Lett. **B79**, 109 (1978).
- [70] Michael Luke and Martin J. Savage, arXiv:hep-ph/9308287v2.
- [71] Voloshin M B, Nucl. Phys. **B154**, 365 (1979).
- [72] Kuang Y P and Yan T M , Phys. Rev. **D41**, 155 (1990).
- [73] Bodwin G T *et. al*, Phys. Rev. **D77**, 094017 (2008).
- [74] Juan-Luis Domenesh-Garret and Miguel-Angel Sanchis-Lozano, Comput. Phys. Commun. **180**, 768 (2009);arXiv:hep-ph/0805.2916v3,arXiv:hep-ph/0805.2704v1.
- [75] Villa S, arXiv:hep-ex/0707.0263v1.
- [76] Link J M *et al.* [FOCUS Collaboration],Phys. Lett. **B586**, 11 (2004).
- [77] Abe K *et al.* [Belle Collaboration], Belle Report BELLE-CONF-0643, hep-ex/0608031.
- [78] Aubert B *et al.* [BaBar Collaboration], Phys. Rev. Lett. **97**, 222001 (2006).
- [79] Artuso M *et al.* [CLEO Collaboration], Phys. Rev. Lett. **95**, 251801 (2005).
- [80] Aubin C *et al.* Phys. Rev. Lett. **95**, 122002 (2006).

Table 10: The leptonic BR of  $D$  and  $D_s$  mesons.

		$\text{BR}_\tau \times 10^{-3}$	$\text{BR}_\mu \times 10^{-4}$	$\text{BR}_e \times 10^{-8}$
$D$	CPP $_\nu$ =0.1	1.5	2.2	0.5
	0.3	1.7	3.6	0.8
	0.5	1.6	4.7	1.1
	0.7	1.3	5.6	1.3
	0.8	1.2	5.9	1.4
	0.9	1.0	6.3	1.5
	1.0	0.9	6.6	1.5
	1.1	0.7	6.9	1.6
	1.3	0.5	7.3	1.7
	1.5	0.3	7.7	1.8
	Expt.[47]	< 2.1	4.4±0.7	
		$\text{BR}_\tau \times 10^{-2}$	$\text{BR}_\mu \times 10^{-3}$	$\text{BR}_e \times 10^{-7}$
$D_s$	CPP $_\nu$ =0.1	4.3	2.5	0.6
	0.3	6.3	4.1	1.0
	0.5	7.4	5.4	1.3
	0.7	8.0	6.4	1.5
	0.8	8.2	6.9	1.6
	0.9	8.3	7.3	1.7
	1.0	8.4	7.7	1.8
	1.1	8.4	8.0	1.9
	1.3	8.4	8.6	2.0
	1.5	8.3	9.1	2.1
	Expt.[47]	6.6±0.6	6.2±0.6	